Journal of Coastal Research	00	0	000–000	Coconut Creek, Florida	Month 0000

Remote-Sensed Mapping of *Sargassum* spp. Distribution around Rottnest Island, Western Australia, Using High-Spatial Resolution WorldView-2 Satellite Data

Tin C. Hoang[†]*, Michael J. O'Leary[†‡], and Ravi K. Fotedar[†]

[†]Department of Environment and Agriculture
Faculty of Science and Engineering
Curtin University
Perth, WA 6102, Australia

[‡]The Western Australian Marine Science Institution
Floreat, WA 6014, Australia

www.cerf-jcr.org

www.JCRonline.org

ABSTRACT

Hoang, T.C.; O'Leary, M.J., and Fotedar, R.K., 0000. Remote-sensed mapping of *Sargassum* spp. distribution around Rottnest Island, Western Australia, using high-spatial resolution WorldView-2 satellite data. *Journal of Coastal Research,* 00(0), 000–000. Coconut Creek (Florida), ISSN 0749-0208.

Satellite remote sensing is one of the most efficient techniques for marine habitat studies in shallow coastal waters, especially in clear waters where field observations can be easily carried out. However, such *in situ* observations have certain limitations: they are time consuming, have a limited ability to capture spatial variability, and require an interdisciplinary approach between marine biologists and remote-sensing specialists. The main objective of this study was to survey and map *Sargassum* beds around Rottnest Island, Western Australia, through a combination of high spatial resolution WorldView-2 imagery, using a validated depth invariant index model for water-column correction, and in-field observations. The combination of field survey data and four classification methods resulted in highly accurate classification outcomes that showed the distribution patterns of *Sargassum* spp. around Rottnest Island during the austral spring season (October 2013). Overall, the minimum distance and Mahalanobis classifiers yielded the highest overall accuracy rates of 98.32% (kappa coefficient, $\kappa = 0.96$) and 98.30% ($\kappa = 0.96$), respectively. The K-means classification method gave the lowest accuracy percentage of 42.50% ($\kappa = 0.22$). Thus, the primary results of this study provide useful baseline information that is necessary for marine-conservation strategic planning and the sustainable utilization of brown macroalgae resources around the Western Australian coast.

ADDITIONAL INDEX WORDS: *Brown macroalgae, satellite remote sensing, coastal habitat mapping.*

INTRODUCTION

The marine brown algae *Sargassum* spp. is an ecologically important genus that has a worldwide distribution and is especially dominant in tropical and shallow subtropical waters (Hanisak and Samuel, 1987; Mattio and Payri, 2011; Mattio *et al.*, 2008). As a living renewable resource, *Sargassum* spp. also has economic value, including potential use in medicines, fertilizer, and biofuel or energy resources and as a carbon offset, whereby it has the ability to both fix and sequester carbon dioxide from the atmosphere and distribute it among the different layers of the ocean (Aresta, Dibenedetto, and Barberio, 2005; Gellenbeck and Chapman, 1983; Hong, Hien, and Son, 2007). As such, there is an increasing need to map the density and spatial distribution of *Sargassum* beds to better quantify the total biomass of this resource.

Marine habitat mapping is usually undertaken using ground surveys and direct visual observations, side-scan sonar, and free diving. All of these techniques are extremely time consuming, expensive, and often unfeasible for large areas (Fearns *et al.*, 2011; Komatsu *et al.*, 2002; Tecchiato *et al.*, 2011). A more cost-effective method that is often employed is satellite remote-sensing imagery (SRSI). It requires fewer field surveys, and with the cost of imagery decreasing with concurrent improvements in spatial and temporal resolution, there has been a rapid increase in the use of SRSI for various marine-mapping applications.

The SRSI method has been successfully applied for mapping marine habitats in shallow coastal waters, especially in clear waters with good light penetration, where it is easy to carry out field observations (Green *et al.*, 2000). A range of satellite imagery tools have been used for mapping the spatial and temporal distribution of macroalgae and their associated habitats, including the Medium Resolution Imaging Spectrometer (Gower *et al.*, 2005), IKONOS (Andréfouët, Zubia, and Payri, 2004; Sagawa *et al.*, 2008, 2010, 2012a; Stumpf, Holderied, and Sinclair, 2003), Satellite Pour l'Observation de la Terre 2/4 (Casal *et al.*, 2011b; Hau, Son, and Mai, 2009), Land Satellite (Vahtmäe and Kutser, 2007), the Compact High Resolution Imaging Spectrometer/Project for On-Board Autonomy (Casal *et al.*, 2011a), and the Advanced Land Observing Satellite–Advanced Visible and Near Infrared Radiometer type 2 (ALOS–AVNIR-2; Phauk *et al.*, 2012; Sagawa *et al.*, 2012b; Tin, Tuan, and Son, 2009).

The recent launch of the commercial WorldView-2 (WV-2) satellite has further increased the spatial and spectral resolution of SRSI, with images with a 0.5-m spatial resolution for the single panchromatic band (450–800 nm) and a 2-m resolution for the eight multispectral bands. In addition to the four standard colors: blue, green, red, and near-infrared 1, WV-

DOI: 10.2112/JCOASTRES-D-15-00077.1 received 2 May 2015; accepted in revision 4 August 2015; corrected proofs received 1 October 2015; published pre-print online 29 October 2015.
*Corresponding author: hoangcongtin@gmail.com

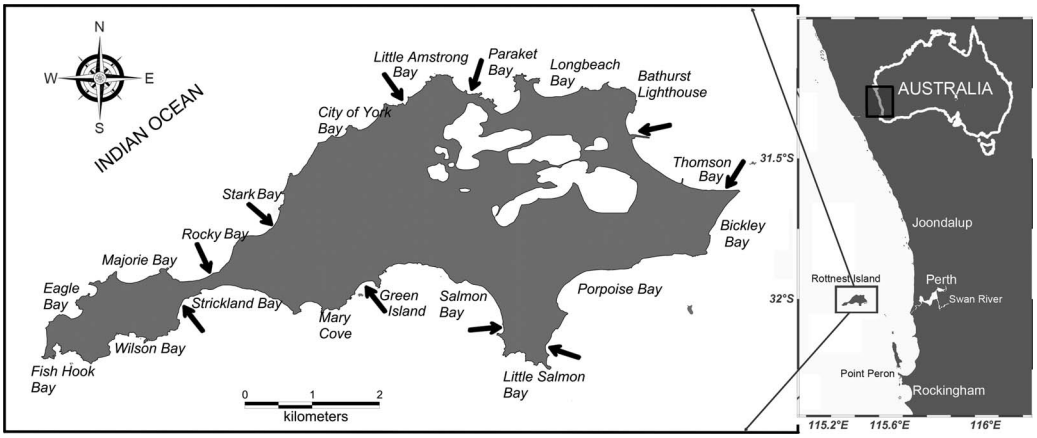

Figure 1. Map of the study area, Rottnest Island (32°00′ S, 5°30′ E), off the WA coast about 19 km west of Fremantle. It is one of the largest class A reserves in the Indian Ocean.

2 includes four new colors, *i.e.* coastal band (400–500 nm), yellow band (585–625 nm), red edge (705–745 nm), and near-infrared 2 (860–1040 nm), which are particularly useful for coastal ecosystem studies (DigitalGlobe Staff, 2013; Updike and Chris, 2010).

The WV-2 satellite has been effectively used to map submerged aquatic vegetation, sea grass, and macroalgae since 2010 (Cerdeira-Estrada *et al*., 2012; Chen *et al*., 2011; Maheswari, 2013; Midwood and Chow-Fraser, 2010; Seoane, Arantes, and Castro, 2012; Soo-Chin and Chew-Wai, 2012). However, no systematic study into the utility of WV-2 imagery for the remote sensing of macroalgae has been performed, particularly of *Sargassum* spp. Fearns *et al*. (2011) reported the application of a hyperspectral remote-sensing model for coastal substrate mapping around Rottnest Island and along the Western Australian (WA) coast, using airborne hyperspectral sensor HyMap data, which was collected along shallow areas of the WA coast during April 2004. Harvey (2009) also used hyperspectral remote sensing in the study of Rottnest Island's substrate habitats. No studies have used multispectral satellite remote sensing to map marine habitats in general or to map canopy macroalgae along the WA southwest coast. Therefore, assessing the distribution of *Sargassum* beds using high spatial resolution images from the WV-2 satellite in this study could be considered the first such approach.

On the shallow subtidal and intertidal reefs around the WA coast, *Sargassum* spp. form a dominant brown macroalgae group that shows strong seasonal variation (Kendrick and Walker, 1991). The highest biomass and density of reproductive thalli are recorded in spring (September to November; Kendrick, 1993; Kendrick and Walker, 1994). According to Kendrick (1993), *Sargassum spinuligerum* in the subtidal zone has an increased density of vegetative thalli from autumn (March–May) to winter (June–August). *Sargassum spinuligerum* reproduces in spring (September–November) and summer (December–February), when it reaches the greatest biomass. In this study, we obtained high-resolution satellite imagery in spring (October 2013) that aimed to capture the highest biomass and density of *Sargassum* spp. surrounding Rottnest Island.

The main objective of this study was to test the utility and ability of WV-2 imagery in the mapping, monitoring, and classification of *Sargassum* beds and associated habitats around Rottnest Island. This was achieved through the combination of ground truth validation and the methodological development of image processing techniques. The present study is expected to contribute to a better understanding of the distribution of *Sargassum* beds and their potential impact on broader ecosystem functions.

METHODS

This study integrates field observations and high spatial resolution WV-2 imagery processing techniques to provide an assessment of coastal marine *Sargassum* beds around Rottnest Island, WA. Field observation methods included free diving, monitoring transect lines, quantify quadrats, and underwater photography techniques. The satellite remote-sensing processing techniques are described later.

Study Area

Rottnest Island is 11 km long and 4.5 km at the widest part, with a total area of about 1900 hectares (Figure 1). Rottnest Island is ecologically unique because it is located at the boundary between tropical and temperate zones, with both temperate and tropical species coinhabiting the marine environment (Rottnest Foundation Staff, 2014). Tropical marine species are sustained by the Leeuwin Current, which transports warm tropical waters south along the WA coastline. This allows the island to host one of the southernmost coral reefs in Australia and in the world. The island's biodiversity is internationally acknowledged as having a high conservation value, consisting of mollusks, sea grasses, macroalgae, coral, and fish species with both tropical and temperate affinities (Rottnest Foundation Staff, 2014). Rottnest Island has become one of the most popular destinations for holiday makers and marine conservation in the WA region and across Australia (Phillip, 1988). All these unique features make Rottnest Island

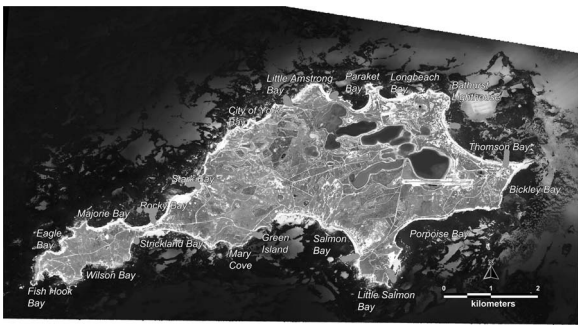

Figure 2. The composite image of WV-2 of Rottnest Island, WA, captured at 0249 (GMT) on 28 October 2013. It shows 100-m field survey transect lines with ground truth locations (•) around Rottnest Island.

an ideal place to study the ecological and spatial distribution of macroalgae in general and *Sargassum* spp. in particular.

Ground Truth of *Sargassum* Beds

Ground truth validation of SRSI was carried out using photoquadrat snorkel surveys. A total of 98 random ground truth points were collected along 10 transect lines that were 100 m long. Field data were collected over a 2-day trip on 21 and 22 September 2013, with two trips after classification or validation being carried out on 24 November 2013 and 14 February 2015.

Each transect line was surveyed for species composition, percentage cover, and thallus height of *Sargassum* spp. (Figure 2). Transect lines were designed to cover the major bays, points, reefs, and sanctuaries around the island (sand, coral, and rocky habitats), as well as to cover a range of water depths. Along each transect line, five 0.5 × 0.5 m quadrants were randomly placed within a 10- to 20-m distance between each quadrat at a bottom depth ranging between 0.5 and 3.5 m. Within each quadrat, the percentage cover of all macroalgae groups including *Sargassum* spp. were measured, as well as the length of five randomly selected *Sargassum* thalli for mean canopy height (MCH), which was measured from the base to the tip of the selected branches. The percentage cover was calculated based on the percentage cover of macroalgae in a quadrat. The quadrat was divided into 25 small square boxes, with each box representing 4% of the cover. For instance, if *Sargassum* covered 10 small boxes within a quadrat, it was indicated with a 40% cover. The mean value of canopy cover for each transect line represents data from random quadrats. Numerous fresh *Sargassum* spp. were collected at these selected study sites and were then stored in plastic bags and transported to Curtin Aquatic Research Laboratories.

Satellite Data Acquisition

Currently, WV-2 satellite imagery is among the highest spatial resolution commercial imagery in the world. The WV-2 satellite was launched into orbit in mid-October 2009 and was fully operational on 6 January 2010 (DigitalGlobe Staff, 2013). The WV-2 imagery used in this study was obtained at 023858 Greenwich mean time (GMT) on 28 October 2013. The WV-2 image was collected during the season that that has shown historically high *Sargassum* spp. biomass cover in the region (Kendrick, 1993; Kendrick and Walker, 1994). The selection of WV-2 images was based on two key factors: (1) captured time that coincided with high *Sargassum* spp. distribution periods (late spring/early summer) and (2) the highest-quality images during cloud-free coverage.

Table 1. *Characteristics of WV-2 multispectral eight-band and panchromatic images acquired at Rottnest Island, WA.*

Imagery Parameters	Multispectral
Acquired date	28 October 2013
Acquired time/local time	023858 GMT/104925 Australia/Perth
Top left coordinate	352,350.00 mE, 462,504.00 mN
Rows/columns	3974/6826
Path	one swathe, 91 km^2
Nadir/off-nadir	Nadir/20° off-nadir
Projection/datum	UTM-50S/WGS84
Processing level	Ortho-Ready Standard Level 2A
Resampling method	Cubic convolution
Data storage format	Geo TIFF
Mean sun elevation/azimuth	65.0°/45.6°
Cloud cover	0%
Band and spatial resolution	2.00 × 2.00 m

TIFF = tagged image file format.

The WV-2 image data are composed of eight bands, six of which are visible; the other two are near-infrared bands with a 2-m spatial resolution (Table 1). Notably, the WV-2 satellite carries a sensor with spectral bands of the coastal band (400–450 nm), which is capable of penetrating into the shallow water column (DigitalGlobe Staff, 2013; Seoane, Arantes, and Castro, 2012; Updike and Chris, 2010). The WV-2 image was georeferenced in the Universal Transverse Mercator (UTM) World Geodetic System 1984 (WGS84), zone 50 south (50S), which used a cubic convolution method for resampling.

WV-2 Image Preprocessing Methods

A flow chart of the analysis processes of mapping macroalgae, other macroalgae groups, and their associated benthic habitats using high-resolution WV-2 imagery is shown in Figure 3.

Geometric Correction

The raw WV-2 satellite images were registered in UTM-50S and converted to geographical longitude and latitude WGS84 data. The satellite images were delivered as a level LV3D product to ensure that they were sensor corrected, radiometrically corrected, and orthorectified (DigitalGlobe Staff, 2013; Eckert, 2012; Liang, Li, and Wang, 2012).

Converting WV-2 Data to Reflectance

Two steps are involved in the conversion of WV-2 data to reflectance values. The first step involves converting the digital number (DN) in the range from 0 to 255 into radiance values, and the second step converts the radiance in watts per square meter per steradian per micron ($W\ m^{-2}\ sr^{-1}\ \mu m^{-1}$) into reflectance values. This process requires relevant input information, such as the distance between the sun and the earth (in astronomical units), the day of the year (Julian date), the mean solar exoatmospheric irradiance, and the solar zenith angle.

DN to Radiance

To convert DN values to radiance values, the gain and offset method was used with these values from the metadata file

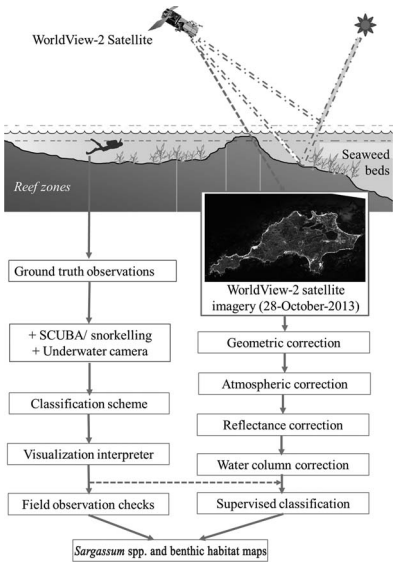

Figure 3. Flow chart of the analysis processes of mapping macroalgae and canopy benthic habitats using high-resolution WV-2 imagery.

(Table 2; Chavez, 1996). The formula to convert DN to radiance using gain and bias values is

$$L_\lambda = \text{gain*DN} + \text{offset} \quad (1)$$

where L_λ is the cell value of the satellite spectral radiance for a given spectral band ($\text{W m}^{-2}\ \text{sr}^{-1}\ \mu\text{m}^{-1}$); the DN is the range of 0 to 255 for a given cell; gain is the gain value for a given specific band, and offset is the bias value for the given specific band. This processing stage was analyzed using the WorldView Radiance calibration toolbox in the environment for visualizing images (ENVI) software package (Exelis, 2014).

Radiance to Top of Atmosphere Reflectance

As mentioned earlier, the distance between the sun and the earth (in astronomical units), the day of the year (Julian date), the mean solar exoatmospheric irradiance, and the solar zenith angle were used to calculate reflectance (NASA, 2011). The top of atmosphere (ToA) is the spectral radiance entering the WV-2's telescope at an altitude of 700 km (Chander, Markham, and Helder, 2009; Updike and Chris, 2010). The following formula for calculating reflectance was used:

$$\rho_\lambda = \pi . L_\lambda . d^2 \Big/ ESUN_\lambda . \cos(SZ) \quad (2)$$

where ρ_λ is the unitless planetary reflectance, L_λ is the spectral radiance for a given spectral band (from Equation (1)), d is the earth–sun distance in astronomical units (Table 3), $ESUN_\lambda$ is the mean solar exoatmospheric irradiance for the given spectral band, and SZ is the solar zenith angle (extracted from metadata files). The step of converting the radiance to ToA can be processed by calibrated radiance at the data-specific utilities in the spectral toolbox in the ENVI 4.7 software (Exelis, 2014).

Atmospheric Correction

The WV-2 satellite spectral data were atmospherically corrected, using the dark substrate method, to reduce haze and other influences of atmospheric and solar illumination. The major principle of the dark substrate method is to calculate the mean value of deepwater pixels (Gordon and McCluney, 1975; Liang, Li, and Wang, 2012; Stumpf, Holderied, and Sinclair, 2003). The atmospheric correction was carried out using the dark substrate tool box in the ENVI 4.7 software (Exelis, 2014).

Water-Column Corrections

This study used the variable depth model derived by Lyzenga (1981) for water-column corrections and is one of the most popular methods when using satellite remote-sensing images for the mapping the marine coastal ecosystems. The depth invariant index (DII) was calculated as follows:

$$DII_{ij} = \ln(L_i) - \frac{k_i}{k_j} * Ln(L_j) \quad (3)$$

where L_i is the measured radiance of a given band i, L_j is the measured radiance of a given band j, and k_i/k_j is the ratio of the attenuation coefficient that is derived from the slope of the log-transformed plot at numerous depths.

Table 2. *Spectral information, spatial resolution, gain and offset, and band-averaged solar spectral irradiance of the WV-2 in Rottnest Island acquired on 28 October 2013.*

				Rottnest Island		SR	
Spectral Bands	SB	SI	EB	Gain	Offset	Nadir	20° Off-Nadir
Panchromatic band	450–800	1580.8140	284.6			0.46	0.52
Eight multispectral bands							
MS1—NIR1	770–895	1069.7302	98.9	0.026229	0.00	1.85	2.07
MS2—red	630–690	1559.4555	57.4	0.013780	0.00		
MS3—green	510–580	1856.4104	63.0	0.026081	0.00		
MS4—blue	450–510	1974.2416	54.3	0.017990	0.00		
MS5—red edge	705–745	1342.0695	39.3	0.017990	0.00		
MS6—yellow	585–625	1738.4791	37.4	0.017990	0.00		
MS7—coastal*	400–450	1758.2229	47.3	0.017990	0.00		
MS8—NIR2	860–1040	861.2866	98.9	0.017990	0.00		

* From Updike and Chris (2010).
SB = spectral band edges (in nanometers), SI = spectral irradiance with unit (in watts per square meter per micron), EB = effective bandwidths $\Delta\lambda$ (in nanometers), SR = sensor resolution (in meters), NIR1 = near-infrared 1, NIR2 = near-infrared 2.

Table 3. *Earth–sun distance in astronomical units.*

Julian Day	Distance
1	0.9832
15	0.9836
32	0.9853
46	0.9878
60	0.9909
74	0.9945
91	0.9993
106	1.0033
121	1.0076
135	1.0109
152	1.0140
166	1.0158
182	1.0167
196	1.0165
213	1.0149
227	1.0128
242	1.0092
258	1.0057
274	1.0011
288	0.9972
305	0.9925
319	0.9892
335	0.9860
349	0.9843
365	0.9833

Masking

To eliminate the spectral variability that is affected by terrestrial and deepwater areas, the vector layer of these areas was masked to the satellite images.

Image Classification and Data Analysis

Field survey data on macroalgae distribution and abundance were processed using the ENVI 4.7 Integrated Development Language remote-sensing software. Four classifiers—the minimum distance, Mahalanobis distance, K-means, and parallelepiped classifiers—were chosen for this study, because they are the most commonly used classifiers in marine coastal habitat mapping studies to date (Andréfouët, Zubia, and Payri, 2004; Belgiu, Drăguţ, and Strobl, 2014; Benfield *et al.*, 2007; Carle, Wang, and Sasser, 2014; Ghosh and Joshi, 2014; Muslim, Komatsu, and Dianachia, 2012). The coastal habitat around Rottnest Island can be categorized into six classes: rocky substrate, sandy, canopy macroalgae (*Sargassum* and *Ecklonia* spp.), red macroalgae, sea grass, and mixed vegetation. The whole analysis process is presented in a diagram in Figure 4, and the scheme for habitat classification is supplied in Table 4.

Accuracy Assessment

Error matrices and Cohen's kappa (κ) were used to assess the accuracy of the classification results. These are helpful models to understand the accuracy of the classification scheme. The κ coefficient can be employed to assess the agreement between classification results and reality (Congalton, 1991). Cohen's kappa is calculated as follows:

$$\kappa = \frac{N\sum_{i=1}^{r} x_{ii} - \sum_{i=1}^{n}(x_{i+} \times x_{+i})}{N^2 - \sum_{i=1}^{n}(x_{i+} \times x_{+i})} \quad (4)$$

The producer and user accuracy indices were also calculated for each classification result (Congalton and Green, 2009). The producer and user accuracy indices are among the most popular indices to evaluate classification outcomes. The producer accuracy is an index that measures the possibility that the classifier fit the image pixel in class A similar to the ground truth in class A. The producer accuracy index is also related to the errors of omission (exclusion; Congalton, 1991; Congalton and Green, 2009). From the user perspective, the user accuracy is an index to measure the possibility that the classifier labeled the image pixel in class A. The overall accuracy and the κ coefficient for the four classification techniques were also evaluated.

RESULTS

This study is the first of its kind to use WV-2 high-resolution multispectral satellite imagery to map *Sargassum* spp. distribution. Eight *Sargassum* spp. have been identified in intertidal and subtidal beds around Rottnest Island. Among these *Sargassum* spp., *S. spinuligerum, S. distichum,* and *S. podacanthum* are most abundant (Kendrick, 1993). However, because of the similarities in morphological structure, includ-

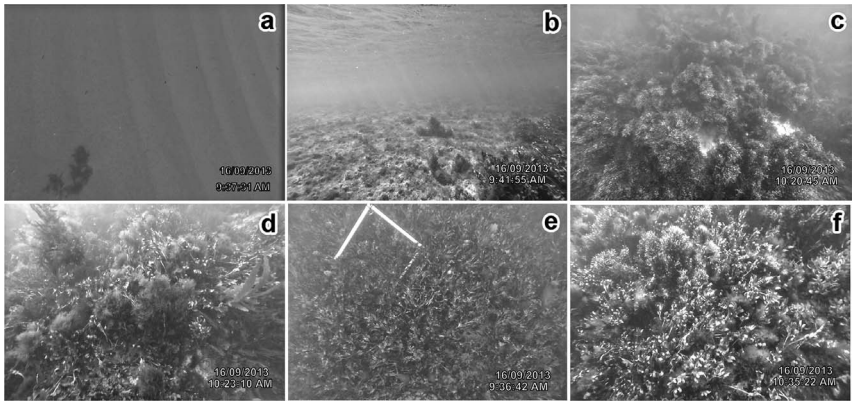

Figure 4. The ground truth survey images taken from the study sites. (a) Sandy substrate, (b) limestone substrate, (c) *Sargassum* spp. habitat, (d) red macroalgae, (e) sea grass *(Amphibolis australis),* (f) algae turf habitat.

Table 4. *Scheme used for habitat classification based on ground truth data.*

Class 1	Class 2	Description	Ground Truth Image
Unvegetated	Sandy substrate	Fine sand with bared substrates	Figure 3a
	Limestone substrate	Bared substrates or some coralline on its surface	Figure 3b
Vegetated	Canopy macroalgae (*Sargassum* and *Ecklonia* spp.)	Most abundant *Sargassum* spp., commonly found in tidal and sublittoral zones and mostly attached to limestone rock	Figure 3c
	Red macroalgae	Red algae (*Gracilaria* sp.) and coralline algae often found in limestone rock, sand, and mud	Figure 3d
	Sea grass	*Amphibolis* sp. often found on sandy substrates in the sublittoral zone; also found on gravel and firm, clay banks	Figure 3e
	Algae turf	Community of green, red, and brown algae	Figure 3f

ing thallus color and length, holdfast shapes, stipe, and primary branches (Kendrick, 1993; Mattio *et al.*, 2008), individual *Sargassum* spp. could not be distinguished or separated spectrally. Therefore, *Sargassum* spp. distribution was defined at the genus level.

Sargassum spp. Percentage Cover and Canopy Height from Field-Survey Data

Percentage Cover of *Sargassum* spp. and Other Macroalgae Groups

In the period between September and November 2013, the spatial distribution of *Sargassum* spp. showed statistically significant differences ($P = 0.008$) in percentage cover between monitored transect lines around Rottnest Island. The highest percentage cover of *Sargassum* spp. was found on the inshore reefs at depths of 0.5 to 3.5 m in the areas around Salmon Bay, Rocky Bay, and Armstrong Bay, with values of 61.6 ± 11.5, 53.3 ± 13.1, and 48.3 ± 14.3%, respectively. The percentage cover in Parakeet Bay and Green Island area was 45.9 ± 24.0 and 18.9 ± 10.5%, respectively. The lowest percentage cover of *Sargassum* spp. was found in the Parker Point area (15 ± 5.7%), and Thomson Bay had a cover of 4.3 ± 0.0% (Figure 5).

For other macroalgae groups, *Ecklonia* sp. in particular, statistically significant differences ($P = 0.041$) were observed between monitored transect lines. The greatest percentage cover was found for Green Island, Thomson Bay, Parker Point, and Rocky Bay, with values of 77.8 ± 10.2, 59.3 ± 0.0, 51.3 ± 13.4, and 42.8 ± 13.2%, respectively. The lowest percentage cover of other macroalgae groups was found in the Parakeet Bay, Armstrong Bay, and Salmon Bay, with values of 40.9 ± 24.0, 36.7 ± 9.4, and 17.9 ± 6.4%, respectively.

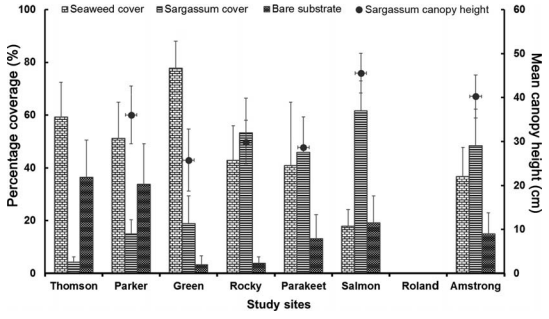

Figure 5. The percentage coverage and canopy height of *Sargassum* spp. observed from different sites during spring 2013. Thomson = Thomson Bay, Parker = Porpoise Bay (Parker Point), Green = Green Island, Rocky = Rocky Bay, Parakeet = Parakeet Bay, Salmon = Salmon Bay, Roland = Strickland Bay (Roland Smith Memorial), Armstrong = Little Armstrong Bay. Each column shows the mean and standard error of five observed quadrats (0.5 × 0.5 m).

Canopy Height

There were no statistically significant differences ($P = 0.069$) between the monitored transect lines in terms of MCH. The MCH of *Sargassum* spp. was highest along the monitored transect line in Salmon Bay (45.5 ± 4.5 cm). Armstrong Bay, Parker Point, and Rocky Beach had MCH values of 4.9 ± 40.3, 36.1 ± 6.54, and 29.8 ± 4.9 cm, respectively. The lowest MCH of 25.8 ± 0.6 cm was found in Green Island.

Separating *Sargassum* spp. and Other Macroalgae Groups

Spectral profile analysis of the major substrate types and biological communities around Rottnest Island showed that there was a significant difference between limestone and sand substrates and among *Sargassum* spp., *Ecklonia* sp., algae turf, and sea grass communities (Figure 6). The characteristically different spectral profiles between the major substrate types and the biological communities enable the *Sargassum* spp. distribution to be mapped.

Comparing the spectral profiles of bare sand and limestone rock, sand has higher and increasing reflectance intensity across the 400- to 750-nm spectrum than does limestone rock, for which the reflectance decreases after 650 nm and has peaks at 500, 550, and 650 nm. In addition, it is rare to encounter bare limestone rock, and the reflectance value is probably influenced by encrusting and turf algae. The substrate reflectance components are significantly different when compared with the spectral reflectance of biological communities, such as *Sargassum* spp., *Ecklonia* sp., algal turf, and sea grass (Figures 6a and b).

Sargassum and *Ecklonia* spp. have a similar bimodal spectral reflectance pattern, with a first weak-intensity peak at 600 nm and the lowest value at 650 nm, with the change of reflection direction. The major difference between the two species is the overall intensity: *Ecklonia* sp. exhibits higher peak values of 0.05 at the 600-nm wavelength, whereas *Sargassum* spp. have the highest spectral reflectance value of 0.02 at 600 nm, which has a lower peak value than for *Ecklonia* sp. (Figures 6e and f).

Algae turf communities can include coralline algae, red algae, green algae, and brown folios algae. The spectral reflectance values of the algae turf communities on Rottnest Island are often dictated by the coralline algae, which have a

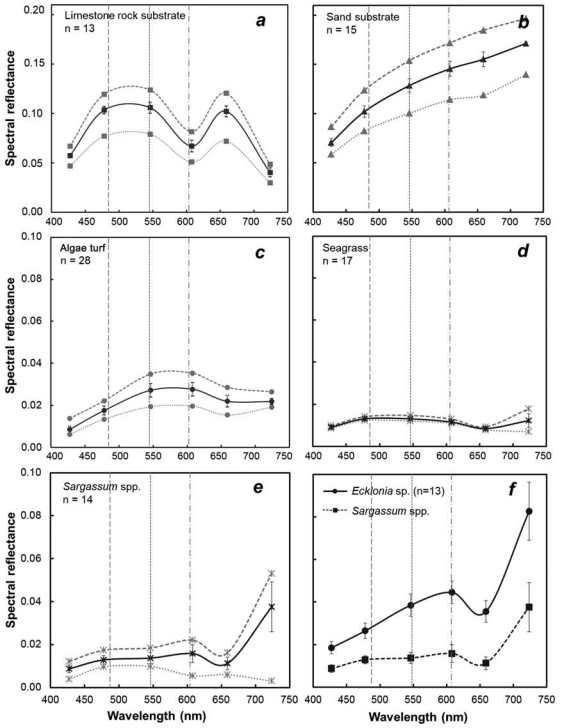

Figure 6. Spectral profiles of most benthic components extracted from WV-2 imagery. (a) Limestone substrate, (b) sand substrate, (c) algae turf (coralline algae, red algae, green algae, and brown algae), (d) sea grass; (e) *Sargassum* spp., (f) *Ecklonia vs*. *Sargassum* spp.

high cover abundance and irradiance value peaking between 550 and 600 nm (Figure 6c).

The three main sea grass species distributed around Rottnest Island are *Posidonia* sp., *Amphibolis* sp., and *Halophila* sp., among which *Posidonia* sp., and *Amphibolis* sp. have the most abundant distributions. Because of the similarity of spectral profiles in the present study, we classified all three sea grass species into one group. These species have the highest reflectance irradiance values between 500 and 550 nm (Figure 6d).

Spatial Distribution of *Sargassum* spp. from Satellite Remote-Sensing Data

The combined results of the three-band match with red edge, red edge, and yellow bands showed that the macroalgae beds with a majority of *Sargassum* spp. were detected by yellow and orange patterns. The following environmental and biological factors helped to detect the *Sargassum* spp. bed boundaries: (1) the beds are found in clear waters and in shallow intertidal and subtidal zones (0.5–10 m); (2) *Sargassum* spp. and other brown macroalgae (*Ecklonia* and *Cystoseira* spp.) show a preference for rocky substrates, *i.e*. not sandy, which cannot be confused with sea grass on a sandy substrate; and (3) *Sargassum* spp. have different spectral characteristics compared to other seaweed groups that are highly distinct in the high-resolution WV-2 imagery (2 m; Figure 6).

Satellite remote-sensing WV-2 data showed the highest densities of *Sargassum* spp. around Rottnest Island along the shallow subtidal zone on limestone substrates. The area around Green Island contained patches of high *Sargassum* spp. coverage, but the distribution of *Sargassum* spp. in this area was not even and was instead concentrated mainly around fringing reefs (Figure 7). In Little Armstrong Bay and Stark Bay areas, the distribution of macroalgae was also high and was concentrated in large meadows on the right side and the outside of the fringing reefs. The area had red patterns, which supposedly symbolize submerged coral reef platforms.

Accuracy Assessment

The accuracy assessment method was employed to test four classifiers: the minimum distance, Mahalanobis, K-means, and parallelepiped methods. The minimum distance method produced the greatest classification accuracy results for the seawater class followed by accuracy rates for *Sargassum* spp., sand, and coral reef of 99.8, 97.8, 81.8, and 75.5%, respectively. The highest accuracy rates obtained by the Mahalanobis classification method were found in the seawater class (99.6%), followed by *Sargassum* spp. (98.1%), sand (80.3%), and coral reef (78.1%). The classification results produced by the parallelepiped classification method were 95.7% for seawater, 99.1% for sand, 96.1% for *Sargassum* spp., and 7.5% for coral reef. Of the four classification methods, the K-means method produced the lowest accuracy rates for seawater (45.6%), *Sargassum* spp. (34.5%), and coral reef (0%), but yielded the highest accuracy rate for sand (100; Table 5).

DISCUSSION

To date, no studies on the use of WV-2 images for mapping *Sargassum* spp., particularly along the Australian coast, have been performed. This study showed a high level of accuracy in classifying *Sargassum* spp. using WV-2 imagery, highlighting the utility of SRSI in mapping shallow marine environments. The integrated study of high-resolution satellite data provides useful and valuable information for natural resource managers to respond to questions of seasonal change in *Sargassum* spp. biomass and the typical substrate used by *Sargassum* spp. (Andréfouët, Zubia, and Payri, 2004).

However, benthic habitat mapping using the object-based and supervised classification technique is still subject to a number of limitations, *i.e*. the method requires the gathering of ground truth data. Field data collection is relatively time consuming and expensive (Komatsu *et al*., 2002; Muslim, Komatsu, and Dianachia, 2012; Vahtmäe and Kutser, 2013). In addition, field data do not always correlate with satellite image data because of discrepancies in spatial resolution, time lag between photos and surveys, field survey techniques, and effects due to the environmental conditions of data collection (Kutser, Miller, and Jupp, 2006). In terms of ground truth, this study found that a minimum of 10 transects with five survey quadrats per transect, for a total survey area of approximately 20 km^2, is required for a high-accuracy assessment. Moreover, this study recommends a survey quadrat size of 0.5×0.5 m, which is the standard method for general benthic habitat mapping studies (*e.g*., Duarte and Kirkman, 2001; Japar, Bandeira, and Milchakova, 2001; McKenzie, Finkbeiner, and

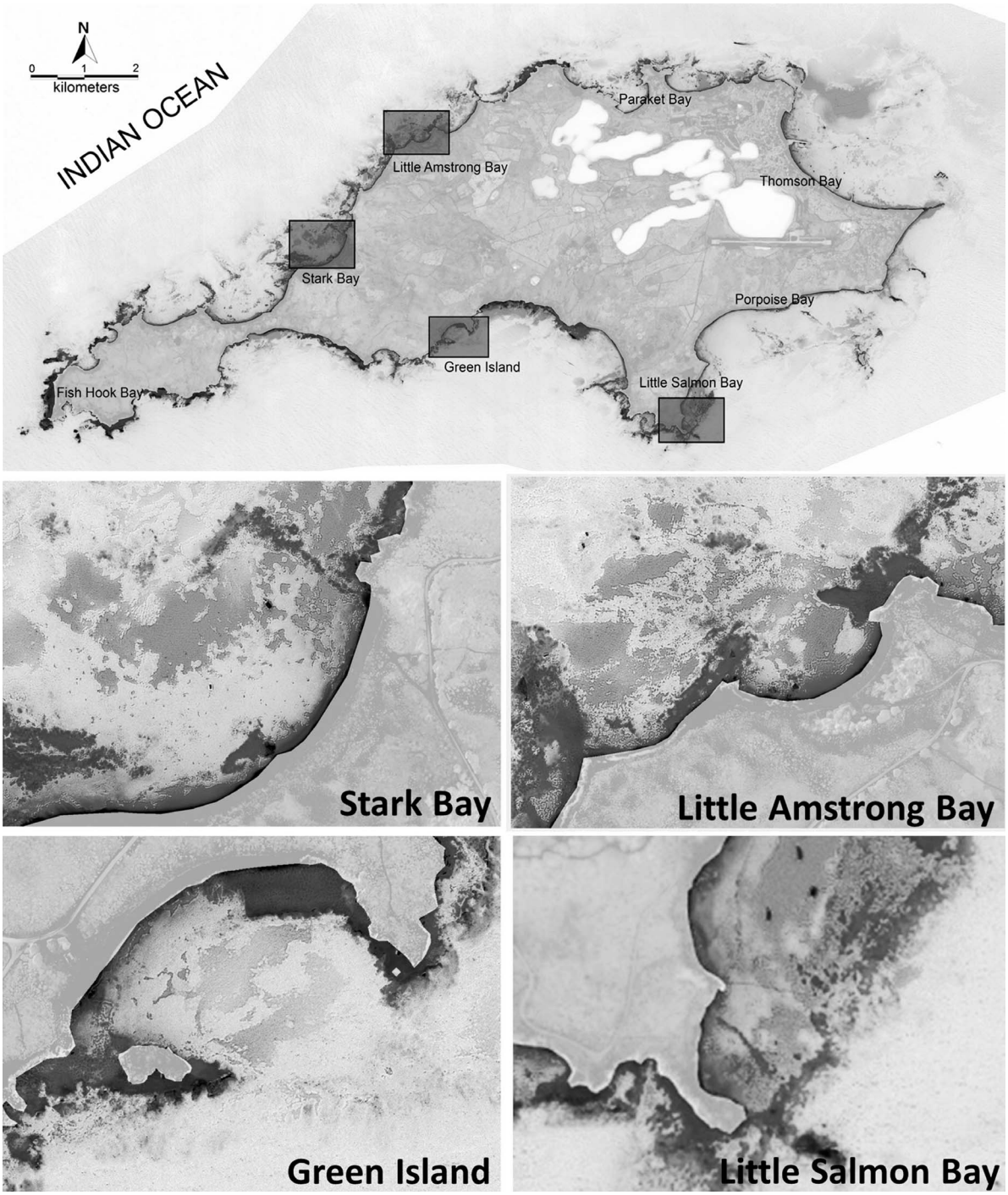

Figure 7. The result of spectral math of the three red edge, red edge, and yellow bands showed the visibly observed distribution of *Sargassum* beds with yellow pixels and red color for submerged reefs around the study sites. (Color for this figure is available in the online version of this paper.)

Kirkman, 2001; Short and Duarte, 2001). We believe that this approach returns better accuracy assessments than numerous previous studies that merely employed the manta tow technique for the photography of the benthic substrate (<0.25 m^2 per site; *e.g.*, Noiraksar *et al.*, 2014).

In addition, this study highlights the importance of understanding seasonal variations in *Sargassum* spp. biomass and distribution before acquiring WV-2 image data. Spring was chosen for this study, because it is when the biomass and cover of *Sargassum* spp. peak in Rottnest Island. Thus, it is

Table 5. *Confusion matrix for WV-2 classification of Rottnest Island Reserve using four classifiers. The accuracy assessment was based on selected main habitats from WV-2 images.*

		Test Areas/Ground Truth (%)				
Classes	Classifiers	Seawater	Sand	*Sargassum*	Coral Reef	Total
Unclassified	MiL	0	0	0	0	0
	MaH	0	0	0	0	0
	KM	0	0	0	0	0
	PAR	4.3	0.9	2.9	3.3	3.9
Seawater	MiL	99.8	0	0.2	0.1	70.6
	MaH	99.6	0	0.1	0.3	70.4
	KM	45.6	0	0.5	0.1	32.3
	PAR	95.7	0	0	0.1	67.6
Sand	MiL	0	81.8	0	21.2	2.0
	MaH	0	80.4	0	18.5	1.9
	KM	0.3	100	65.2	99.7	20.9
	PAR	0	99.1	0.2	85.7	4.1
Sargassum	MiL	0	0	97.8	3.2	24.4
	MaH	0	0	98.1	3.2	24.5
	KM	2.8	0	34.4	0.3	10.5
	PAR	0	0	96.1	3.5	24.0
Coral reef	MiL	0.2	18.2	2.1	75.5	3.0
	MaH	0.4	19.7	1.8	78.1	3.2
	KM	51.4	0	0	0	36.3
	PAR	0	0.1	0.8	7.5	0.4
Total	MiL	100	100	100	100	100
	MaH	100	100	100	100	100
	KM	100	100	100	100	100
	PAR	100	100	100	100	100

MiL = minimum distance, MaH = Mahalanobis, KM = K-means, PAR = parallelepiped.

important to understand the seasonality of *Sargassum* spp. so that WV-2 imagery captures the period of highest biomass and facilitates the mapping of *Sargassum* spp. There is additional value in investigating the utility of WV-2 image data to track and understand the seasonal variations in *Sargassum* spp. biomass and distribution.

One limitation of this study is that it has yet to assess the comparable classification results of the VW-2 pan-sharpened and broad-spectral bands. Likewise, a potential error that might be encountered in the study of coastal ecosystems is the

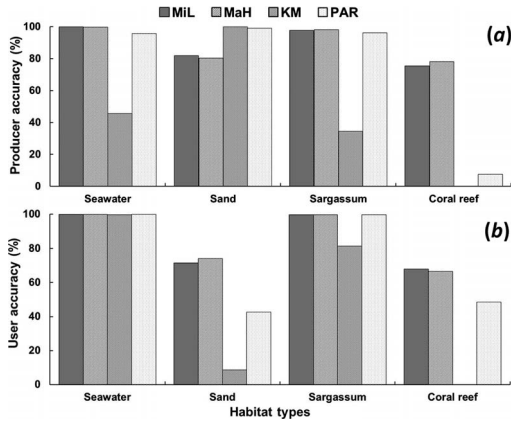

Figure 8. Validation accuracy for each habitat type from different classifiers. (a) Producer accuracy results, (b) user accuracy. MiL = minimum distance, MaH = Mahalanobis, KM = K-means, PAR = parallelepiped.

Table 6. *Confusion matrix of the overall accuracy of the classification maps obtained from the WV-2 image.*

Classification Methods	Overall Accuracy (%)	Kappa Coefficient (κ)
Minimum distance	98.32	0.96
Mahalanobis	98.30	0.96
K-means	42.50	0.22
Parallelepiped	93.50	0.86

variation in the inherent optical properties (IOPs) of the water column. For example, coastal waters are often affected by runoff, upwelling, and water mixing, which can lead to high concentrations of phytoplankton, inorganic particles, and colored dissolved organic matter (CDOM). A change in the IOPs affects both the shape and the magnitude of the reflectance spectra (Vahtmäe and Kutser, 2013). Therefore, further work is required to evaluate the differences in classification results between pan-sharpened and broad-spectral bands and other very high-resolution remote-sensing data (*e.g.*, hyperspectral images and aerial photography) and to assess the potential effect of changing the IOP conditions.

Producer and user accuracies were employed and compared among the four classification techniques of this study (Figure 8). The advantages of the coastal (400–450 nm) and yellow (585–625 nm) bands were illustrated by the high classification accuracy of these types of habitats (Table 6). These are the unique bands that are only found in WV-2 images. With these bands, WV-2 images can penetrate through the clear water column and gather appropriate information about bottom habitats in shallow waters. A similar study by Su, Liu, and Heyman (2008) showed that in the water sector, green light (500–600 nm) can reach a maximum depth of 15 m, red light (600–700 nm) can penetrate to 5 m, and infrared light (700–800 nm) can reach to 0.5 m (Green *et al.*, 2000; Su, Liu, and Heyman, 2008). The overall classification accuracies achieved in the present study are higher than those found by Noiraksar *et al.* (2014), who mapped *Sargassum* beds in Chon Buri province, Thailand, using ALOS–AVNIR-2 images. They used minimum distance and supervised maximum likelihood classification methods, which resulted in overall accuracy rates of 67 and 69%, respectively. However, a study by Carle, Wang, and Sasser (2014), which mapped the distribution of freshwater marsh species using WV-2 imagery, showed that maximum likelihood classifiers delivered the highest overall classification accuracy (75%). They also found that the coastal blue and red edge bands played a major role in enhancing vegetation mapping.

Comparing the classification results of this study with those of previous studies on the *Sargassum* group showed that our study results have a higher classification accuracy ratio (Table 7). This can be explained by two factors. First, as discussed earlier, this study was evaluated source imaging at high spatial resolution (2 m) and spectral resolution (eight bands). In particular, the coastal band is capable of deeply penetrating and gathering appropriate information from marine habitats. Second, our study area (Rottnest Island, which is situated 20 km offshore) has clear ocean waters with a relatively low influence of coastal sediments and nutrients. Consequently, the clearness of the water column is high because of low

Table 7. *Studies that have used WV-2 and other high spatial resolution satellite imagery to map coastal ecosystem and habitat vegetation since October 2010.*

Location	Depth (m)	Satellite Imagery	Employed Techniques and Methods	Identified Habitats	Overall Habitat Map Accuracy	Cited*
Offshore island of Singapore	0–0.8	WV-2 (eight bands)	Unsupervised classification and contextual editing	Sea grass meadow, mangroves, coral reefs	n.a.	(1)
Singapore coastal waters	0.1–20	WV-2 (eight bands)	Computed reflectance spectra of SAV	SAV, sea grasses	Possible to detect SAV in low-turbidity water (up to 25 NTU)	(2)
Recife de Fora, Brazil	n.a.	WV-2, including coastal blue band	Back-and-forth shifting by selecting red–green–blue triplets generates polygons; inverse distance weighted model	Coral reef system, sea grass and macroalgae, coralline algae, coral and octocoral, zooanthidean	Map of coral reef and benthic habitat at 1:5000 scale	(3)
Gulf of Mannar, India	n.a.	WV-2, including coastal blue band	Atmospheric correction, radiance conversion, ToA reflectance	Water, sea grass, island, coral reef	n.a.	(4)
Almería coast (southern Spain)	n.a.	GeoEye-1 and WV-2	Sensor models and geometric quality assessment tests	Assessing geometric accuracy	n.a.	(5)
Wax Lake delta, U.S.	n.a.	WV-2, IKONOS, OrbView-3	MLC and SVM classifiers	Freshwater marsh species	75% for MLC from WV-2 images	(6)
Dukuduku, South Africa	n.a.	WV-2 (eight bands)	Object- and pixel-based classification	Subtropical coastal forest	86.9% ($\kappa = 0.82$)	(7)
Darwin, Australia	n.a.	WV-2 and aerial photographs	Object-based image analysis and SVM classifiers	Mangrove species classification	89% ($\kappa = 0.86$)	(8)

* Literature cited: (1) Chen *et al.*, 2011; (2) Soo-Chin and Chew-Wai, 2012; (3) Seoane, Arantes, and Castro, 2012; (4) Maheswari, 2013; (5) Aguilar, Saldaña, and Aguilar, 2013; (6) Carle, Wang, and Sasser, 2014; (7) Malahlela, Cho, and Mutanga, 2014; (8) Heenkenda *et al.*, 2014.

n.a. = not available, SAV = submerged aquatic vegetation, NTU = nephelometric turbidity units, MLC = maximum likelihood classification, SVM = support vector machine.

concentrations of phytoplankton, inorganic particles, and CDOM in the water. According to Vahtmäe and Kutser (2013), in clear ocean waters, optical remote sensing can be limiting at a depth of 30 m. However, the spectrum of information that is most useful to separate the substrate components is achieved at a depth of 5 to 6 m. Likewise, another study in an open-sea area showed that benthic plants cannot be identified at a bottom depth below about 5 m (Vahtmäe *et al.*, 2012). In this study, therefore, the detection range of *Sargassum* spp. lies within the depth range from 0.5 to 3.5 m and is wholly useful spectral information. In addition, the findings of this study agree with those of Vahtmäe and Kutser (2013), who showed that the classification outcomes from the object-based methods provide higher-quality benthic habitat maps than did the spectral library method (Vahtmäe and Kutser, 2013).

CONCLUSIONS

This study has increased understanding of the spatial distribution of *Sargassum* spp. macroalgae beds around coastal area of Rottnest Island, WA, using field survey and remote-sensing techniques. Based on the results, we conclude that eight-band high-resolution multispectral WV-2 satellite imagery has great potential for mapping and monitoring *Sargassum* beds, as well as associated coastal marine habitats. The results are relevant for coastal marine health monitoring and economic planning purposes on the WA coast using high-resolution satellite imagery with large-scale coverage. However, further study to detect the biomass of *Sargassum* beds, using WV-2 in combination with *in situ* observation data, is required.

ACKNOWLEDGMENTS

The authors thank the Rottnest Island Authority for providing access to the study area and the Department of Parks and Wildlife, WA, for field sampling permission for this research. We are indebted to Anthony Cole and Ngoc Nguyen for their assistance in collecting ground truth data. We acknowledge the anonymous reviewers for their constructive comments. This work was supported partly by the Australia Awards administered by the Department of Foreign Affairs and Trade, Australian Government, and partly by the Curtin Aquatic Research Laboratory, Curtin University.

LITERATURE CITED

Aguilar, M.A.; Saldaña, M.M., and Aguilar, F.J., 2013. Assessing geometric accuracy of the orthorectification process from GeoEye-1 and WorldView-2 panchromatic images. *International Journal of Applied Earth Observation and Geoinformation,* 21, 427–435.

Andréfouët, S.; Zubia, M., and Payri, C., 2004. Mapping and biomass estimation of the invasive brown algae *Turbinaria ornata* (Turner) J. Agardh and *Sargassum mangarevense* (Grunow) Setchell on heterogeneous Tahitian coral reefs using 4-meter resolution Ikonos satellite data. *Coral Reefs,* 23(1), 26–38.

Aresta, M.; Dibenedetto, A., and Barberio, G., 2005. Utilization of macro-algae for enhanced CO_2 fixation and biofuels production: Development of a computing software for an LCA study. *Fuel Processing Technology,* 86(14–15), 1679–1693.

Belgiu, M.; Drăguţ, L., and Strobl, J., 2014. Quantitative evaluation of variations in rule-based classifications of land cover in urban neighbourhoods using WorldView-2 imagery. *ISPRS Journal of Photogrammetry and Remote Sensing,* 87, 205–215.

Benfield, S.L.; Guzman, H.M.; Mair, J.M., and Young, J.A.T., 2007. Mapping the distribution of coral reefs and associated sublittoral habitats in Pacific Panama: A comparison of optical satellite sensors and classification methodologies. *International Journal of Remote Sensing,* 28, 5047–5070.

Carle, M.V.; Wang, L., and Sasser, C.E., 2014. Mapping freshwater marsh species distributions using WorldView-2 high-resolution multispectral satellite imagery. *International Journal of Remote Sensing,* 35(13), 4698–4716.

Casal, G.; Kutser, T.; Domínguez-Gómez, J.A.; Sánchez-Carnero, N., and Freire, J., 2011a. Mapping benthic macroalgal communities in the coastal zone using CHRIS-PROBA mode 2 images. *Estuarine, Coastal and Shelf Science,* 94(3), 281–290.

Casal, G.; Sánchez-Carnero, N.; Sánchez-Rodríguez, E., and Freire, J., 2011b. Remote sensing with SPOT-4 for mapping kelp forests in turbid waters on the south European Atlantic shelf. *Estuarine, Coastal and Shelf Science,* 91(3), 371–378.

Cerdeira-Estrada, S.; Heege, T.; Kolb, M.; Ohlendorf, S.; Uribe, A.; Muller, A.; Garza, R.; Ressl, R.; Aguirre, R.; Marino, I.; Silva, R., and Martell, R., 2012. Benthic habitat and bathymetry mapping of shallow waters in Puerto Morelos reefs using remote sensing with a physics based data processing. *Proceedings of the IEEE International Geoscience and Remote Sensing Symposium* (Munich, Germany), pp. 4383–4386.

Chander, G.; Markham, B.L., and Helder, D.L., 2009. Summary of current radiometric calibration coefficients for Landsat MSS, TM, ETM+, and EO-1 ALI sensors. *Remote Sensing of Environment,* 113(5), 893–903.

Chavez, P.S.J., 1996. Image-based atmospheric corrections—Revisited and improved. *Photogrammetric Engineering & Remote Sensing,* 62(9), 1025–1036.

Chen, P.; Liew, S.C.; Lim, R., and Kwoh, L.K., 2011. Mapping coastal ecosystems of an offshore landfill island using WorldView-2 high resolution satellite imagery. *Proceedings of the 34th International Symposium on Remote Sensing of Environment* (Sydney, Australia), pp. 767–769.

Congalton, R.G., 1991. A review of assessing the accuracy of classifications of remotely sensed data. *Remote Sensing of Environment,* 37(1), 35–46.

Congalton, R.G. and Green, K., 2009. *Assessing the Accuracy of Remotely Sensed Data: Principles and Practices,* 2nd edition. New York: CRC Press, 200p.

DigitalGlobe Staff, 2013. *The Benefits of the 8 Spectral Bands of WorldView-2*: *Applications Whitepaper*. London: DigitalGlobe, *Technical Report WP-8SPEC Rev 01/13,* 12p.

Duarte, C.M. and Kirkman, H., 2001. Chapter 7—Methods for the measurement of seagrass abundance and depth distribution. *In:* Short, F.T. and Coles, C.A.S.G. (eds.), *Global Seagrass Research Methods*. Amsterdam: Elsevier Science, pp. 141–153.

Eckert, S., 2012. Improved forest biomass and carbon estimations using texture measures from WorldView-2 satellite data. *Remote Sensing,* 4(4), 810–829.

Exelis Visual Information Solutions, 2014. *ENVI Products*. http://www.exelisvis.com.

Fearns, P.R.C.; Klonowski, W.; Babcock, R.C.; England, P., and Phillips, J., 2011. Shallow water substrate mapping using hyperspectral remote sensing. *Continental Shelf Research,* 31(12), 1249–1259.

Gellenbeck, K.W. and Chapman, D.J., 1983. Seaweed uses: The outlook for mariculture. *Endeavour,* 7(1), 31–37.

Ghosh, A. and Joshi, P.K., 2014. A comparison of selected classification algorithms for mapping bamboo patches in lower Gangetic plains using very high resolution WorldView 2 imagery. *International Journal of Applied Earth Observation and Geoinformation,* 26, 298–311.

Gordon, H.R. and McCluney, W.R., 1975. Estimation of the depth of sunlight penetration in the sea for remote sensing. *Applied Optics,* 14(2), 413–416.

Gower, J.; King, S.; Borstad, G., and Brown, L., 2005. Detection of intense plankton blooms using the 709 nm band of the MERIS imaging spectrometer. *International Journal of Remote Sensing,* 26(9), 2005–2012.

Green, E.P.; Mumby, P.J.; Edwards, A.J., and Clark, C.D., 2000. Remote sensing handbook for tropical coastal management. *In:* Edwards, A.J. (ed.), *Coastal Management Sourcebooks* 3, Paris: UNESCO, x+316p.

Hanisak, M.D. and Samuel, M.A., 1987. Growth rates in culture of several species of *Sargassum* from Florida, U.S.A. *Hydrobiologia,* 151–152(1), 399–404.

Harvey, M.; Kobryn, H.T.; Beckley, L.E.; Heege, T.; Hausknecht, P., and Pinnel, N., 2007. Mapping the shallow marine benthic habitats of Rottnest Island, Western Australia. *Proceedings of the 3rd EARSeL Workshop Remote Sensing of the Coastal Zone* (Bolzano, Italy).

Hau, L.N.; Son, T.P.H., and Mai, V.X., 2009. Application of remote sensing techniques to detect the distribution of *Sargassum* meadows in coastal waters of Khanh Hoa province. *Proceedings of the National Conference on Marine Biology and Sustainable Development* (Hanoi, Vietnam), pp. 574–580.

Heenkenda, M.; Joyce, K.; Maier, S., and Bartolo, R., 2014. Mangrove species identification: Comparing WorldView-2 with aerial photographs. *Remote Sensing*, 6(7), 6064–6088.

Hong, D.; Hien, H., and Son, P., 2007. Seaweeds from Vietnam used for functional food, medicine and biofertilizer. *Journal of Applied Phycology,* 19(6), 817–826.

Japar, S.B.; Bandeira, S.O., and Milchakova, N.A., 2001. Chapter 11—Methods to measure macroalgal biomass and abundance in seagrass meadows. *In:* Short, F.T. and Coles, C.A.S.G. (eds.), *Global Seagrass Research Methods*. Amsterdam: Elsevier Science, pp. 223–235.

Kendrick, G.A., 1993. *Sargassum* beds at Rottnest Island: Species composition and abundance. *Proceedings of the 5th International Marine Biological Workshop: The Marine Flora and Fauna of Rottnest Island, Western Australia* (Perth, Australia), pp. 455–472.

Kendrick, G.A. and Walker, D.I., 1991. Dispersal distances for propagules of *Sargassum spinuligerum* (Sargassaceae, Phaeophyta) measured directly by vital staining and venturi suction sampling. *Marine Ecology Progress Series,* 79, 133–138.

Kendrick, G.A. and Walker, D.I., 1994. Role of recruitment in structuring beds of *Sargassum* spp. (Phaeophyta) at Rottnest Island, Western Australia. *Journal of Phycology,* 30(2), 200–208.

Komatsu, T.; Chiaki, I.; Ken-ichi, T.; Masahiro, N.; Tomonori, H., and Asahiko, T., 2002. Mapping of seagrass and seaweed beds using hydro-acoustic methods. *Fisheries Science,* 68, 580–583.

Kutser, T.; Miller, I., and Jupp, D.L.B., 2006. Mapping coral reef benthic substrates using hyperspectral space-borne images and spectral libraries. *Estuarine, Coastal and Shelf Science,* 70(3), 449–460.

Liang, S.; Li, X., and Wang, J., 2012. Geometric processing and positioning. *In:* Liang, S.; Li, X., and Wang, J. (eds.), *Techniques Advanced Remote Sensing: Terrestrial Information Extraction and Applications*. Boston: Academic Press, pp. 33–74.

Lyzenga, D.R., 1981. Remote sensing of bottom reflectance and water attenuation parameters in shallow water using aircraft and Landsat data. *International Journal of Remote Sensing,* 2(1), 71–82.

Maheswari, R., 2013. Mapping the under water habitat related to their bathymetry using Worldview-2 coastal, yellow, rededge, NIR-2 satellite imagery in Gulf of Mannar to conserve the marine resource. *International Journal of Marine Science,* 3(11), 91–97.

Malahlela, O.; Cho, M.A., and Mutanga, O., 2014. Mapping canopy gaps in an indigenous subtropical coastal forest using high-resolution WorldView-2 data. *International Journal of Remote Sensing,* 35(17), 6397–6417.

Mattio, L.; Dirberg, G.; Payri, C., and Andréfouët, S., 2008. Diversity, biomass and distribution pattern of *Sargassum* beds in the south west lagoon of New Caledonia (South Pacific). *Journal of Applied Phycology,* 20(5), 811–823.

Mattio, L. and Payri, C., 2011. 190 years of *Sargassum* taxonomy, facing the advent of DNA phylogenies. *The Botanical Review,* 77(1), 31–70.

McKenzie, L.J.; Finkbeiner, M.A., and Kirkman, H., 2001. Chapter 5—Methods for mapping seagrass distribution. *In:* Short, F.T. and

Coles, C.A.S.G. (eds.), *Global Seagrass Research Methods*. Amsterdam: Elsevier Science, pp. 101–121.

Midwood, J. and Chow-Fraser, P., 2010. Mapping floating and emergent aquatic vegetation in coastal wetlands of eastern Georgian Bay, Lake Huron, Canada. *Wetlands,* 30(6), 1141–1152.

Muslim, A.M.; Komatsu, T., and Dianachia, D., 2012. Evaluation of classification techniques for benthic habitat mapping. *In:* Robert, J.F.; Naoto, E.; Delu, P., and Toshiro, S. (eds.), *Proceedings of SPIE Remote Sensing of the Marine Environment II* (Kyoto, Japan), pp. 85250W1–85250W9.

NASA (National Aeronautics and Space Administration), 2011. *Landsat 7 Science Data Users Handbook*. Washington, D.C.: U.S. National Aeronautics and Space Administration Publication, 168p.

Noiraksar, T.; Shuhei, S.; Sophany, P., and Komatsu, T., 2014. Mapping *Sargassum* beds off the coast of Chon Buri Province, Thailand, using ALOS AVNIR-2 satellite imagery. *Botanica Marina,* 57(5), 367–377.

Phauk, S.; Komatsu, T.; Sawayama, S., and Noiraksar, T., 2012. Marine habitat mapping: Using ALOS AVNIR-2 satellite image for seagrass beds at Rabbit (Koh Tonsay) Island, Cambodia. *In:* Robert, J.F.; Naoto, E.; Delu, P., and Toshiro, S. (eds.), *Proceedings of SPIE Remote Sensing of the Marine Environment II* (Kyoto, Japan), pp. 85250V1–85250V6.

Phillip, E.P., 1988. *Guidebook to the geology of Rottnest Island, Excursion Guidebook*. Perth, Western Australia: Geological Society of Australia, Western Australian Division, 67p.

Rottnest Foundation Staff, 2014. *Rottnest Foundation—Conserving the Essence of Rottnest*. http://www.rottnestfoundation.org.au.

Sagawa, T.; Boisnier, E.; Komatsu, T.; Mustapha, K.B.; Hattour, A.; Kosaka, N., and Miyazaki, S., 2010. Using bottom surface reflectance to map coastal marine areas: A new application method for Lyzenga's model. *International Journal of Remote Sensing,* 31(12), 3051–3064.

Sagawa, T.; Mikami, A.; Aoki, M.N., and Komatsu, T., 2012a. Mapping seaweed forests with Ikonos image based on bottom surface reflectance. *In:* Robert, J.F.; Naoto, E.; Delu, P., and Toshiro, S. (eds.), *Proceedings of SPIE Remote Sensing of the Marine Environment II* (Kyoto, Japan), pp. 85250Q1–85250Q7.

Sagawa, T.; Mikami, A.; Komatsu, T.; Kosaka, N.; Kosako, A.; Miyazaki, S., and Takahashi, M., 2008. Mapping seagrass beds using Ikonos satellite image and side scan sonar measurements: A Japanese case study. *International Journal of Remote Sensing,* 29(1), 281–291.

Sagawa, T.; Watanabe, T.; Watanuki, A.; Koike, T.; Kamimura, H., and Komatsu, T., 2012b. Can ALOS-3/HISUI detect seaweed beds more precisely than ALOS/AVNIR-2? *In:* Robert, J.F.; Naoto, E.; Delu, P., and Toshiro, S. (eds.), *Proceedings of SPIE Remote Sensing of the Marine Environment II* (Kyoto, Japan), pp. 85250Y1–85250Y9.

Seoane, J.C.S.; Arantes, R.C.M., and Castro, C.B., 2012. Benthic habitat mapping at Recife de Fora, Brazil: Imagery and GIS. *Proceedings of the 12th International Coral Reef Symposium* (Cairns, Australia), pp. x1–x5.

Short, F.T. and Duarte, C.M., 2001. Chapter 8—Methods for the measurement of seagrass growth and production. *In:* Short, F.T. and Coles, C.A.S.G. (eds.), *Global Seagrass Research Methods*. Amsterdam: Elsevier Science, pp. 155–182.

Soo-Chin, L. and Chew-Wai, C., 2012. Detecting submerged aquatic vegetation with 8-band WorldView-2 satellite images. *Proceedings of IEEE International Geoscience and Remote Sensing Symposium* (Munich, Germany), pp. 2560–2562.

Stumpf, R.P.; Holderied, K., and Sinclair, M., 2003. Determination of water depth with high-resolution satellite imagery over variable bottom types. *Limnology Oceanography,* 48(2), 547–556.

Su, H.; Liu, H., and Heyman, W.D., 2008. Automated derivation of bathymetric information from multi-spectral satellite imagery using a non-linear inversion model. *Marine Geodesy,* 31(4), 281–298.

Tecchiato, S.; Parnum, I.; Collins, L., and Gavrilov, A., 2011. Using multi-beam echosounder backscatter data to map sediments and seagrass. *Proceedings of the 4th International Conference and Exhibition on Underwater Acoustic Measurements: Technologies & Results* (Kos, Greece), pp. 1679–1685.

Tin, H.C.; Tuan, N.Q., and Son, T.P.H., 2009. Utilization of the Advanced Land Observation Satellite (ALOS) imagery and geographical information system (GIS) in evaluating plant cover in Huong Phong commune, Huong Tra district, Thua Thien Hue province. *Proceedings of the Symposium of Application GIS in Natural Resources and Environment Studies* (Hue City, Vietnam), pp. 192–199.

Updike, T. and Chris, C., 2010. *Radiometric Use of WorldView-2 Imagery*. Longmont, Colorado: DigitalGlobe, 17p.

Vahtmäe, E. and Kutser, T., 2007. Mapping bottom type and water depth in shallow coastal waters with satellite remote sensing. *In:* Lemckert, C. (ed.), *Proceedings of the 9th International Coastal Symposium* (Gold Coast, Australia), Journal of Coastal Research, Special Issue No. 50, pp. 185–189.

Vahtmäe, E. and Kutser, T., 2013. Classifying the Baltic Sea shallow water habitats using image-based and spectral library methods. *Remote Sensing,* 5, 2451–2474.

Vahtmäe, E.; Kutser, T.; Kotta, J.; Pärnoja, M.; Möller, T., and Lennuk, L., 2012. Mapping Baltic Sea shallow water environments with airborne remote sensing. *Oceanology,* 52(6), 803–809.